Journal of Materials Chemistry B

Accepted Manuscript

ROYAL SOCIETY OF CHEMISTRY

www.rsc.org/materialsB

Journal Name

ARTICLE

Photo-controlled host–guest interaction as a new strategy to improve the preparation of "breathing" hollow polymer nanospheres as controlled drug delivery

Received 00th January 20xx,
Accepted 00th January 20xx

DOI: 10.1039/x0xx00000x

www.rsc.org/

Haitao Zhang, Wei Tian,* Rongtian Suo, Yang Yue, Xiaodong Fan, Zhen Yang, Hui Li, Wanbin Zhang, and Yang Bai

This paper presents the photo-controlled host–guest interaction between azobenzene and β-cyclodextrin as a new strategy to improve the method for core removal to prepare poly((itaconoyloxy)ethyl methacrylate)-block-poly(N-isopropylacrylamide-based hollow nanospheres. This improved method for the preparation of hollow nanospheres is simple, environment friendly, and highly efficient. The resulting hollow nanospheres displayed a typical "breathing" behavior, which further induces the controlled release of doxorubicin hydrochloride. Cellular toxicity evaluation indicated that the hollow nanospheres possess good biocompatibility and can be used as a promising doxorubicin hydrochloride carrier.

Introduction

Over the past few decades, hollow polymer nanospheres have attracted considerable interest owing to their wide array of applications in chemistry, biotechnology, and materials science.[1-6] Various methods, such as self-assembly of block or graft copolymers in selective solvent,[7-10] layer-by-layer deposition of polyelectrolytes on a template,[11-14] miniemulsion polymerization[15] and polymerization from template,[16-18] have been developed to fabricate hollow nanospheres. Among these methods, the template-assisted approach, also called core removal method, is usually employed in the preparation of hollow nanospheres.[19] In this method, the shell need to cost sacrificial core particles (e.g., gold or silica) with polymer shell layers, and the inorganic and organic cores are removed from the solid nanospheres. However, this method exhibits several intrinsic disadvantages, such as low product yield, resulting from the multistep synthetic process and the lack of structural robustness of the shells upon core removal.[20] In addition, the core removal requires special highly toxic solvent (e.g., HF and THF), leading to the decreased biocompatibility of the resulting hollow nanospheres.[21, 22] Therefore, developing an effective method for core removal in preparing hollow nanospheres remains a challenge.

Herein, we propose a new strategy to improve the core removal method for the preparation of hollow nanospheres by introducing photo-controlled host–guest interaction. The *trans*- and *cis*-isomers of azobenzene (AZO) can be reversibly switched under light irradiation.[23] However, compared with the *cis*-AZO, the *trans*-AZO is well recognized by β-cyclodextrin (β-CD) through hydrophobic and van der Waals interactions. This host–guest interaction between AZO and β-CD is fully reversible under alternating UV and visible light irradiation.[24, 25] Therefore, this photo-controlled host–guest interaction between AZO and β-CD is a simple and environment-friendly method of preparing hollow nanospheres. AZO- and β-CD-containing supramolecular amphiphilies have been investigated as photo-responsive vesicles and nanospheres.[26, 27] However, no work has yet reported on utilizing photo-controlled host–guest interaction to improve the core removal method for the preparation of hollow nanospheres.

Based on our previous work on the β-CD-based host-guest supramolecular chemistry,[28-30] here we use the photo-controlled host–guest interaction as a new strategy to improve core removal method for preparing poly((itaconoyloxy)ethyl methacrylate)-*b*-poly(N-isopropylacrylamide) (PIEMA-*b*-PNIPAM)-based hollow nanospheres. This preparation involves three steps, namely, construction of supramolecular block copolymer *via* host–guest interaction between AZO and β-CD, preparation of shell cross-linked solid nanospheres, and removal of core component by dissociating the host–guest interaction (Schemes 1a–1c). The resulting hollow nanospheres display a typical "breathing" characteristic, indicating that these hollow nanospheres will swell or shrink when subjected to external stimuli, such as temperature or pH.[31, 32] This "breathing" characteristic of the hollow nanospheres can further induce the controlled release of

The Key Laboratory of Space Applied Physics and Chemistry, Ministry of Education and Shanxi Key Laboratory of Macromolecular Science and Technology, School of Science, Northwestern Polytechnical University, Xi'an, 710072 (P. R. China). E-mail: happytw_3000@nwpu.edu.cn

† Electronic Supplementary Information (ESI) available: See DOI: 10.1039/x0xx00000x

doxorubicin hydrochloride (DOX • HCl) when the solution temperature increases up to the lower critical solution temperature (LCST) of PNIPAM (Schemes 1c–1e).

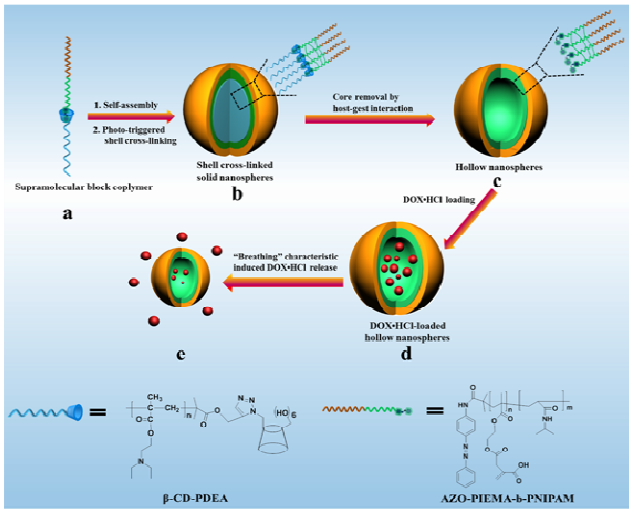

Scheme 1. Preparation and controlled release of doxorubicin hydrochloride (DOX•HCl) of poly((itaconoyloxy)ethyl methacrylate)-*b*-poly(N-isopropylacrylamide) (PIEMA-b-PNIPAM)-based hollow nanospheres. (a–b) Preparation of solid nanospheres can be conducted by two steps as follows. Firstly, the self-assembly of supramolecular block copolymers by the host–guest interaction between azobenzene (AZO) in AZO-PIEMA-*b*-PNIPAM and β-cyclodextrin (β-CD) in β-CD-terminated poly(2-(diethy-lamino)ethyl methacrylate) (β-CD-PDEA); secondly, the photo-triggered shell cross-linking under 253 nm UV light radiation; (b–c) preparation of hollow nanospheres through core removal induced by the dissociation of host–guest interaction between AZO and β-CD under 365 nm UV light radiation; (c–d) DOX•HCl-loaded hollow nanospheres; and (d–e) "breathing" characteristic-triggered DOX•HCl release.

Experiments

Materials

Mono-6-deoxy-6-azido-β-cyclodextrin (β-CD-N_3) and Propargyl 2-Bromoisobutyrate (PBIB) were synthesized according to the literatures, respectively.[33,34] Aminoazobenzol (AZO, 99%,) and 2-Bromo-2-methylpropionyl bromide (BP, 98%,) were purchased from ACROS Chemical Industries (USA). N,N,N′,N′′,N′′-pentamethyldiehylenetriamine (PMDETA) and 2-Hydroxy-4′-(2-hydroxyethoxy)-2-methylpropiophenone (IRGACURE® 2959) were supplied by Yu tian Chemical (Liyang City, China) and used as received without further purification. Tris(2-(dimethylamino)ethyl)amine (Me_6TREN), copper (I) bromide (CuBr, 98%), Itaconic anhydride (IA) (97%), 2-(Diethyl amino)-ethyl methacrylate (DEA, 99%), 2-Hydroxyethyl methacrylate (HEMA，98%) and Propargyl alcohol (98%) were purchased from Aldrich. N-isopropylacrylamide (NIPAM，98%) was purchased from TCI. Doxorubicin hydrochloride (DOX·HCl, 99%) was purchased from Sigma. Triethylamine (TEA) and dichloromethane (DCM) were dried over CaH_2 and distilled prior to use. All other reagents were purchased from Sinopharm Chemical Reagent Co. and used as received.

Methods

^{1}H-NMR was recorded on a Bruker-Avance III NMR spectrometer (400 MHz) with dimethyl sulfoxide-d_6 (DMSO-d_6) and D_2O as solvents. The 2D ^{1}H-NMR NOESY spectra were recorded on a Bruker-Avance III NMR spectrometer (400 MHz) with D_2O as solvent (1.0 M NaOD or CF_3COOD was used for adjusting the solution pH). An isothermal titration calorimeter (ITC; Micro Cal Inc., U.S.A.) has been used for determining the single titration curve of the interaction between AZO and β-CD, and the equilibrium constant corresponding to the formation of a complex between those species. UV-vis spectrophotometer measurement was performed on Shimadzu UV-2550 modelspectroscopy (Shimadzu, Japan). Size and distribution of samples were measured by Zetasizer Nano-ZS dynamic light scattering (DLS) (Malvern Instruments, UK). Each sample was kept at a predetermined temperature for 3 min before measurement without any filter. Slight light scattering (SLS) analysis was performed on a DAWN HELEOS-Ⅱ multi-angle light scattering detector (Wyatt Technology Corporation, USA) operated at 665 nm, using Gallium-arsenic as incident laser beam source. SLS data were collected at 6 different concentrations of the aggregates and 18 different angles for each concentration. The data were analyzed on HELEOS-Ⅱ. Firmware 2.4.0.4 Advanced software to determine R_g. TEM was performed on JEM-2010 microscope (Japan) with an electron kinetic energy of 300 kV. The samples were prepared by aspirating thesolutions (0.5 mg/mL) on to the carbon-coated copper grids at the same setting time. Excessive solution was adsorbed away with filter paper after 10 min, and then the samples were measurment without any negative staining.

Synthesis of aminoazobenzol-ended poly(2-hydroxyethyl methacrylate)-block-poly(N-isopropylacrylamide) (AZO-PHEMA-*b*-PNIPAM)

Atom transfer radical polymerization (ATRP) polymerization has frequently been used to prepare block copolymers due to the precise control of polymerization with various monomers.[35] The diblock copolymer AZO-PHEMAA-*b*-PNIPAM was synthesized via successive ATRP polymerization of HEMA and NIPAM, and subsequent esterification between Itaconic anhydride (IA) and hydroxyl groups in PHEMA units (**Scheme S1**). The detailed synthesis and characterization of AZO-PIEMA-*b*-PNIPAM was described in the Supporting Information (Fig. S1–S3 and Table S1).

Synthesis of β-cyclodextrin-terminated poly(2-(diethylamino)ethyl methacrylate) (β-CD-PDEA)

β-CD-PDEA was prepared via ATRP of DEA monomer using β-CD-Br as the initiator and CuBr/PMDETA as catalysts (Scheme S2). The detailed synthesis and characterization of AZO-PIEMA-

b-PNIPAM and β-CD-PDEA were described in the Supporting Information (Fig. S4 and S5).

Synthesis of PDEA-*b*-PIEMA-*b*-PNIPAM

The supramolecular block copolymer PDEA-*b*-PIEMA-*b*-PNIPAM was constructed through inclusion complexation between AZO-PIEMA-*b*-PNIPAM and β-CD-PDEA at pH 6.0. In a typical example, β-CD-PDEA (20 mg) and equivalent molar AZO-PIEMA-*b*-PNIPAM were dissolved 1 ml pH 6.0 HCl, respectively. Under vigorous stirring, AZO-PIEMA-*b*-PNIPAM solution was added into β-CD-PDEA solution via a syringe pump at a flow rate of 0.2 mL/min.

Preparation and "breathing" property of PIEMA-*b*-PNIPAM-based hollow nanospheres

PIEMA-*b*-PNIPAM-based hollow nanospheres were prepared by a sequential process of shell cross-linked solid nanospheres and removal of core under UV light irradiation. Firstly, PDEA-*b*-PIEMA-*b*-PNIPAM solution (20 mmol/mL, pH 6.0) was dialysised (M_w cut-off, 3.5 kDa) against pH 9 NaOH solution for 24 h and then 5.6 mg 2-Hydroxy-4'-(2-hydroxyethoxy)-2-methylpropiophenone (IRGACURE® 2959) was added. After that addition, the mixed solution was irradiated 10 min with 253 nm UV light, the mixed solution was dialysised against deionized water for 24 h and the fresh deionized water was replaced approximately every 6 h. Stock solutions with a characteristic bluish tinge were typically obtained. Shell cross-linked PDEA-*b*-PIEMA-*b*-PNIPAM-based nanospheres were then obtained by freeze drying. After that, the above product (5 mg) was dissolved into 2 ml pH 6.8 HCl at room temperature and dialysised (M_w cut-off, 2000 kDa) against fresh deionized water under irradiation of 365 nm UV light. After 48 h, the dialyzed solution was adjusted to 10 mL to obtain PIEMA-*b*-PNIPA-based hollow nanospheres solution for further experiments. "Breathing" property of the hollow nanospheres was tested as following. Firstly, the size trend of the hollow nanosphers (0.5 mg/mL) was tested as the temperature was increased and decreased between 25 and 40°C. The morphology of hollow nanospheres at 25 and 37 °C was tested by TEM.

Drug Loading and release of hollow nanospheres

The obtained hollow nanospheres (50 mg) were added into the DOX•HCl solution (5 mL, 1.0 mg/mL, pH = 7.4). After 24 h, the DOX•HCl-loaded hollow nanospheres were centrifuged to remove the free excess DOX•HCl molecules. Then the drug concentration in the supernatant solution was analyzed using a UV spectrophotometer at a wavelength of maximum absorbance (480 nm) after being diluted. The drug loading capacity of the hollow microspheres was calculated from the drug concentrations in solutions before and after adsorption.

In vitro drug release profiles were obtained using a dynamic dialysis method. The release experiments were conducted at 25 and 37 °C. Typically, DOX•HCl-loaded hollow nanospheres solution with 100 mg mL^{-1} equivalent DOX concentration was placed into a dialysis bag and introduced to 50 mL of phosphate buffered saline (PBS; 0.1 mol L^{-1}, pH = 7.4) with magnetic stirring at 200 rpm. At hourly intervals, 3 mL samples were removed from the release medium, and the same volume and temperature of fresh PBS was added to the release medium. The accumulated drug release of DOX was determined using UV-vis measurement.

Cell Experiments

The cellular toxicity of the hollow nanospheres was tested as following. A2780 human ovarian carcinoma cancer cells were seeded in a clear 24-well plate at a density of 2×10^4 cells/well in 1000 μL of complete RPMI 1640 and 10% fetal calf serum (FCS) and grown for 6 h with 5% CO_2 at 37 °C. A2780 cells were subsequently incubated with and without the hollow nanospheres. The ultimate concentration of hollow nanospheres was 0.5 mg/mL. After another 24, 48, and 72, of incubation, the number of living cells in every group was measured. The number of living cells is expressed as the mean ± standard deviation, and a *t* test was used for statistical analysis of the data. Differences were considered statistically significant when the P value was less than 0.05.

MTT cell proliferation assay was used to evaluate the cytotoxicities of DOX•HCl-loaded hollow nanospheres. A2780 cells were seeded at a density of 1×10^4 cells/well in 96-well transparent plate and incubated for 24 h at 37 °C. All growth medium were prepared by supplementing RPMI 1640 and 10% FCS. The medium was then replaced by the free DOX•HCl and DOX • HCl-loaded hollow nanospheres at various drug concentrations from 0.01 to 12.8 μg/mL in the medium. They were then incubated for another 48 h before replacing the medium with 0.1mL of fresh growth medium and 20 μL of MTT solution. After incubation for another 4 h, the culture medium was removed and 150 mL DMSO was added. The plates were vigorously shaken before measuring the relative color intensity using a microplate reader at 480 nm. Cell viability for that particular concentration of sample was expressed as a percentage of the intensity of the controls ± standard deviation. Each experiment was repeated 3 times at each concentration. Another group subjected to same free DOX•HCl, DOX•HCl-loaded hollow nanospheres cultured at 25 °C was used as control.

Results and discussion

Synthesis of supramolecular block copolymer PDEA-*b*-PIEMA-*b*-PNIPAM

The supramolecular block copolymer PDEA-*b*-PIEMA-*b*-PNIPAM was first constructed through host–guest inclusion complexation between AZO-PIEMA-*b*-PNIPAM and β-CD-PDEA in aqueous solution with pH 6.0. The detailed synthesis and characterization of AZO-PIEMA-*b*-PNIPAM and β-CD-PDEA were described in the Supporting Information (Fig. S1–S5 and Table S1). The host–guest interaction of PDEA-*b*-PIEMA-*b*-PNIPAM was confirmed using 2D ^{1}H NMR NOESY and ITC (Fig. 1 and 2). Fig. 1A shows the 2D ^{1}H NMR NOESY spectra of an equimolar solution of AZO-PIEMA-*b*-PNIPAM (10 mM) and β-CD-PDEA (10 mM) in D_2O at pH 6.0 and 25 °C, which proves

that the signals of *trans*-AZO protons are correlated with those of β-CD's inner protons. The signals at δ 7.4-7.9 ppm belonged to the AZO moieties of AZO-PIEMA-*b*-PNIPAM shown strong cross-peaks arising from dipolar interactions with the signals at 3.8 ppm ascribed to the H-3 and H-5 protons located within the cavity of β-CD moieties of β-CD-PDEA. This phenomenon strongly indicates that AZO moieties were deeply embedded within the β-CD cavities. The 2D ^{1}H NMR NOESY spectra of PDEA-*b*-PIEMA-*b*-PNIPAM solution (Fig. 1B) revealed the disappearance of the correlation peaks between the protons of AZO and the inner protons of β-CD following a 365 nm UV light irradiation, indicating the dissociation of PDEA-*b*-PIEMA-*b*-PNIPAM. Because the *trans*-AZO in the solution transformed into the *cis* form as revealed by the photoisomerization following the 365 nm UV irradiation.[23] Subsequently, ITC experiments were performed to measure the binding affinity directly. In a typical experiment, the aqueous solution of AZO-PIEMA-*b*-PNIPAM (12.0 mM) was trickled into the β-CD-PDEA solution (0.6 mM), and an exothermic binding isotherm was obtained. The data yielded a binding constant (K) of 1.18×10^3 M^{-1} less than that of the simple AZO/β-CD complex (5.3×10^3 M^{-1}) (Fig. 2).[36] It has been reported that lower K_t indicated that the inclusion complex is easy to be dissociated under some stimuli.[37] Therefore, the reduced interaction force induced rapid UV light-induced dissociation.[25] We further discovered that the supramolecular pseudo-block copolymers contain a nearly 1:1 stoichiometry of AZO and β-CD. Thus, a supramolecular block copolymer was successfully prepared on the basis of the above results.

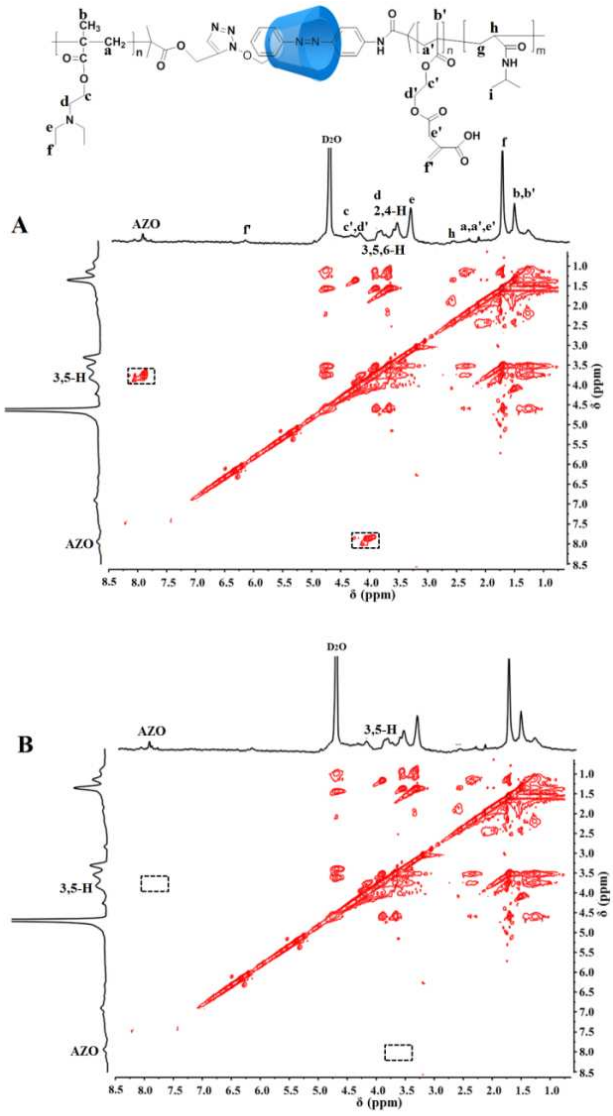

Fig. 1 2D ^{1}H NMR NOESY spectra of an equimolar solution of AZO-PIEMA-*b*-PNIPAM (10 mM) and β-CD-PDEA (10 mM) before (A) and after (B) 365 nm UV light irradiation at pH 6.0 and 25°C.

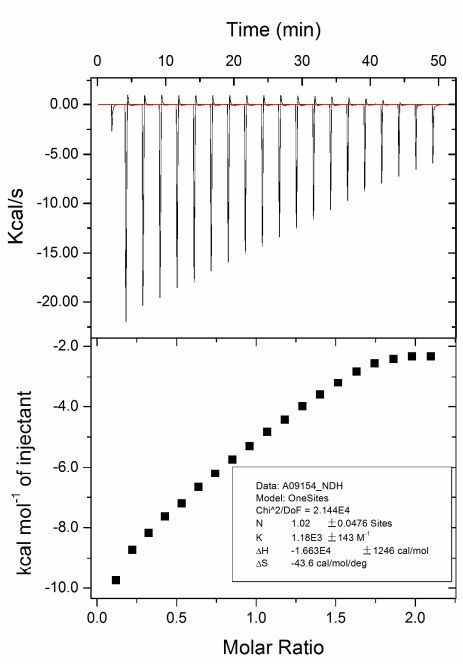

Fig. 2 Typical ITC data corresponding to the binding interaction of AZO-PIEMA-*b*-PNIPAM (12.0 mM) with β-CD-PDEA (0.6 mM) in pH 6.0 HCl solution at 25 °C. Up panels show exothermic heat flows that are released upon successive injection of 10 μL aliquots of AZO-PIEMA-*b*-PNIPAM into β-CD-PDEA. Down panels show integrated heat data, giving a differential binding curve which was fit to a standard single-site binding model.

Preparation of PDEA-*b*-PIEMA-*b*-PNIPAM-based solid nanospheres

Firstly, PDEA-*b*-PIEMA-*b*-PNIPAM-based solid nanospheres were prepared by a sequential self-assembly of PDEA-*b*-PIEMA-*b*-PNIPAM in aqueous solution and photo-triggered cross-linking of C=C double bond in the shell layer (Schemes 1a–1b). The solubility of PDEA is caused by the protonation of tertiary amine residues at pH<6; however, PDEA becomes water-insoluble in neutral or alkaline solutions.[38] By contrast, PNIPAM and PIEMA are both water soluble at alkaline pH. Therefore, PDEA-*b*-PIEMA-*b*-PNIPAM is an amphiphilic copolymer and can self-assemble into nanospheres under alkaline condition.[39] Compared with other cross-linking methods, byproducts are not formed in nearly all photo-cross-linking.[40] Thus, UV light was used to trigger the opening of the C=C double bond for further shell cross-linking of the solid nanospheres (Schemes 1a–1b).

The size and morphology of solid nanospheres were determined through transmission electron microscopy (TEM), dynamic light scattering/static light scattering (DLS/SLS), and ^{1}H NMR in D_2O. TEM results indicated that the self-assembling solid nanospheres exhibit an average diameter (D_{av}) of 212 nm at pH 9.**0** (Fig. 3A), and the size nearly did not change when the shell layer of the solid nanospheres was cross-linked (Fig. 3C). Similarly, DLS analysis revealed that the Z-average diameter (D_z)

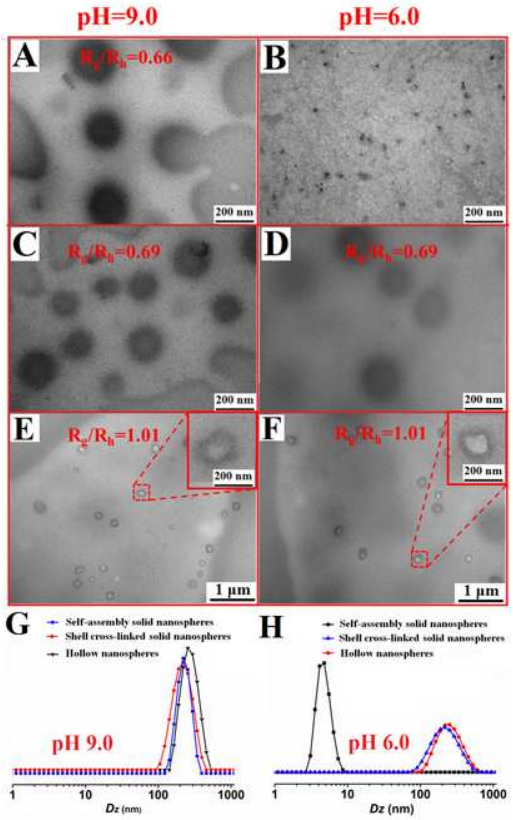

Fig. 3. TEM images (A–F) and DLS results (G–H) of various nanospheres at pH 9.0 (left column) and 6.0 (right column). Self-assembling solid nanospheres at (A) pH 9.0 and (B) pH 6.0; shell cross-linked solid nanospheres at (C) pH 9.0 and (D) pH 6.0; and hollow nanospheres at (E) pH 9.0 and (F) pH 6.0. Typical intensity-averaged diameter distributions of various nanospheres in aqueous solutions (0.5 mg/mL) with (G) pH 9.0 and (H) pH 6.0 at 25 °C.

values of the solid nanospheres with and without shell cross-linking are nearly similar (214 and 216 nm, respectively) (Fig. 3G), which is consistent with the TEM results. Additionally, the ratio of radius of gyration to hydrodynamic radius (R_g/R_h), which were based from the DLS/SLS results, of the self-assembling and shell cross-linked nanospheres were 0.66 and 0.69, respectively (Table 1), indicating their being solid structures.[41,42] Furthermore, the shell cross-linking was validated by TEM and DLS. When the solution pH was adjusted from 9.0 to 6.0, the self-assembling solid nanospheres nearly disaggregated completely (Fig. 3B), and their D_z was considerably reduced to 5 nm (Fig. 3H)**.** By contrast, the shell cross-linked solid nanospheres maintained their morphology (Fig. 3D) with a stable D_z of 215 nm (Fig. 3H) and R_g/R_h of 0.69. PDEA becomes a typical cationic polyelectrolyte and water soluble at pH 6.0,[43] thereby leading to the disappearance of the amphiphilic property of PDEA-*b*-PIEMA-*b*-PNIPAM. Therefore, the solid nanospheres without shell cross-linking disaggregated, whereas the shell cross-linked solid nanospheres remained stable.

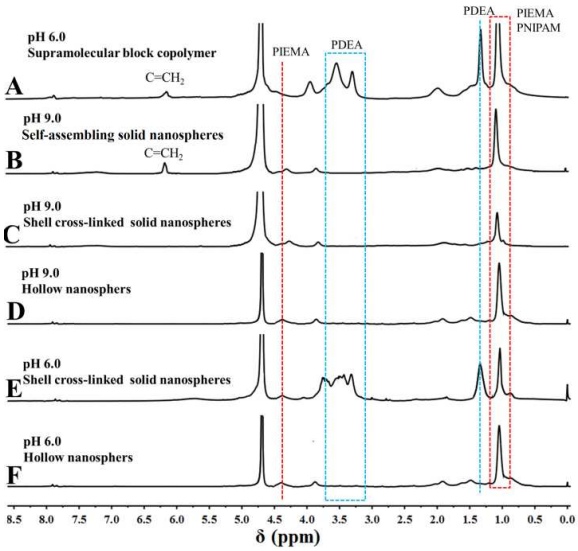

Fig. 4 ^{1}H NMR spectra of the (A) supramolecular block copolymer at pH 6.0 and (B) self-assembling solid nanospheres at pH 9.0, shell cross-linked solid nanospheres at (C) pH 9.0 and (E) pH 6.0, and hollow nanospheres at (D) pH 9.0 and (F) pH 6.0 (1.0 M NaOD or CF_3COOD was used to adjust the solution pH value).

^{1}H NMR analysis was employed to further investigate the structure of the solid nanospheres. Compared with the ^{1}H NMR spectrum of the supramolecular block copolymer at pH 6.0 (Fig. 4A), the ^{1}H NMR spectrum of the self-assembling solid nanospheres at pH 9.0 (Fig. 4B) exhibited the signals of PIEMAA and PNIPAM segments, whereas the proton NMR signals at δ = 3.1 ppm to 3.75 ppm belonging to the hydrophobic PDEA unit were not observed. Furthermore, the peaks at 6.22 ppm of $-C=CH_2$ in the PIEMA moiety disappeared after the 253 nm UV light irradiation (Fig. 4C), while the protons of PDEA appeared again after the pH value was adjusted from 9.0 to 6.0 because the protonated PDEA segment is water soluble at pH 6.0. These results proved that PDEA served as the hydrophobic region, whereas the PIEMA-*b*-PNIPAM chains served as the hydrophilic outer shell. The results also indicated that the shell of the solid nanospheres was cross-linked by the double bond with the PIEMA moiety.

Preparation of PIEMA-*b*-PNIPAM-based hollow nanospheres

Finally, the PIEMA-*b*-PNIPAM-based hollow nanospheres were produced by removing the PDEA core through photo-controlled host–guest interaction (Schemes 1b–1c). On the one hand, owing to the photoisomerization of AZO, the host–guest interaction between AZO and β-CD can be dissociated using 365 nm UV light irradiation.[24] On the other hand, PDEA can be protonated and may be rendered completely water soluble in acidic condition.[43] Therefore, the core and shell components of the shell cross-linked solid nanospheres were separated under 365 nm UV light irradiation at pH 6.0. The protonated PDEA core diffused out of the shell cross-linked solid nanospheres, leading to the formation of a hollow structure. To maintain the structural robustness of the shells upon core removal, the shell cross-linked solid nanospheres were first dispersed into HCl with pH 6.0 and then diarized in deionized water to remove the protonated β-CD-PDEA core. To maintain an accordant testing condition, the pH of the solution containing the obtained hollow nanospheres was then adjusted back to 9.0.

Compared with the dark-colored cores of the shell cross-linked solid nanospheres (Fig. 3C and 3D), the cavities of the hollow nanospheres are light-colored (Fig. 3E and 3F), indicating the removal of the β-CD-PDEA core. This result was further confirmed DLS and SLS (Fig. 3G and 3H); the D_z of the hollow nanospheres was higher than that of the solid nanospheres, which may be due to the fact that the restraint of the PDEA core on the polymer network of the shells was removed and the expanding cross-linked PIEMA that serves as a hydrogel material.[44] In addition, the R_g/R_h of the hollow nanospheres is 1.01 at pH 9.0 and 6.0, which implies that they are vesicular structures.[42]

Table 1 Size and morphology of different nanospheres in aqueous solution (0.5 mg/mL) at 25°C

Sample	D_{av}[a] (nm)		D_z[b] (nm)		PDI[c]		R_g[d] (nm)		R_g/R_h[e]	
	pH 9.0	pH 6.0	pH 9.0	pH 6.0	pH 9.0	pH 6.0	pH 9.0	pH 6.0	pH 9.0	pH 6.0
Self-assembly solid nanospheres	212	-	214	5	0.117	0.451	71	-	0.66	-
Shell cross-linked solid nanospheres	215	216	216	215	0.135	0.128	77	77	0.69	0.69
Hollow nanospheres	225	223	286	287	0.127	0.126	145	145	1.01	1.01

[a)]Average diameter determined by TEM; [b)]Z-average diameter determined by DLS; [c)]DLS-measured diameter based on the polydispersity of particles; [d)]The radius of gyration (R_g is defined as the mass weighted average distance from the centre of mass to each mass element, which was measured by monitoring the angular dependence of the sample scattering intensity in SLS; [e)]The hydrodynamic radius (R_h) , which is measured by DLS, is the representative of the size of a hard sphere that diffuses at the same rate as the particle being measured.

Compared with the ^{1}H NMR spectrum of the shell cross-linked solid nanospheres at pH 6.0 (Fig. 4E), that of the hollow nanospheres did not show the β-CD-PDEA peaks but exhibited the characteristic peaks of PIEMA-*b*-PNIPAM at pH 6.0 (Fig. 4F). These results confirmed that the protonated β-CD-PDEA completely diffused out of the nanospheres resulting from UV light irradiation. Additionally, the 2D NMR analysis was employed to further confirm the removal of the β-CD-PDEA core. The 2D ^{1}H NMR NOESY spectra of the shell cross-linked solid nanospheres in aqueous solution at pH 6.0 revealed disappearance of the correlation peaks between the AZO protons of AZO-PIEMAA-*b*-PNIPAM and inner protons of β-CD following UV light irradiation at 365 nm (Fig. S6). This result further indicates that the β-CD-PDEA dissociated from the shell cross-linked solid nanospheres.

"Breathing" Property of hollow nanospheres

The hollow nanospheres obtained in this study demonstrated a thermo-induced "breathing" behavior owing to the presence of the thermo-responsive PNIPAM segments.[45,46] Fig. 5A shows that when the temperature increased from 25 °C to 37 °C at pH 7.4, the D_z of the hollow nanospheres decreased from 223 nm to 110 nm, whereas the D_z was restored to 220 nm after reducing the temperature to 25 °C. This cycle could be repeated several times (Fig. 5B). TEM further confirmed the changes in size of the hollow nanospheres. The results showed that the size of the hollow nanospheres was 215 nm at pH 7.4 and 25 °C (Fig. 5C), whereas the D_{ov} value decreased to 105 nm at pH 7.4 and 37 °C (Fig. 5D). This highly reversible thermo-induced swelling and shrinkage of the hollow nanospheres prove that the hollow nanospheres exhibit "breathing" behaviors.[31] In this case, the thermo-controlled swelling can be regarded as "breathing in", whereas shrinkage is "breathing out". The similar "breathing" behaviors of hollow nanospheres were also reported by other groups.[47,48]

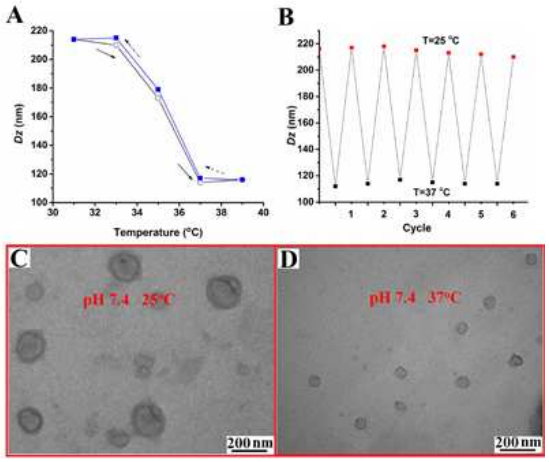

Fig. 5 "Breathing" behavior of the hollow nanospheres rendered by the thermo-responsive PNIPAM segment. (A) Tendency of the hollow nanospheres to change in size as temperature of the solution varies; (B) cyclic changes in D_z values of the hollow nanospheres caused by alternately adjusting the solution temperature between 25 °C and 37 °C at pH 7.4. TEM images of the hollow nanospheres at 25 °C (C) and 37 °C (D) at pH 7.4, respectively.

Controlled drug release and in vitro cytotoxicity of DOX•HCl-loaded hollow nanospheres.

To further confirm the "breathing" behavior of the hollow nanospheres, we investigated the controlled drug release of the hollow nanospheres. We loaded the anticancer drug DOX•HCl into the hollow nanospheres (Fig. S7) and then tested its release profile through *in vitro* dialysis. The time-dependent cumulative release curves of the DOX•HCl-loaded hollow nanospheres were measured using UV–vis spectroscopy at 25 °C and 37 °C at pH 7.4. Fig. 6A shows that the release of DOX•HCl was faster at 37 °C than at 25 °C. This discrepancy may be attributed to two possible reasons. First, the hollow nanospheres were in the "breathing in" state resulting from the collapse of the thermo-responsive PNIPAM chains at 37 °C. The collapse of the PNIPAM layer may have led to the formation of pores or channels throughout the thermo-responsive layer;[49] thus, the permeability of the PNIPAM layer for the guest molecules was enhanced. Second, in the "breathing in" state, the shrinkage of the hollow nanoparticle increased the density of DOX in the cavity, which caused for the rapid release of DOX•HCl. These results clearly indicate that the rate of drug release by the DOX•HCl-loaded hollow nanospheres was temperature-dependent.

Additionally, basic cell experiments were performed to evaluate the cellular toxicity of the hollow nanospheres. The A2780 cells were incubated with and without hollow nanospheres (0.5 mg/mL), and the number of living cells in each group was recorded from day 1 to day 3. Fig. 6B shows that the number of living cells in the vesicle group was statistically equivalent to that in the blank group ($P > 0.05$), and the morphology of the living cells in the vesicle group was also similar to that in the blank group (Fig. 6C and 6D). This demonstrates that the drug-free hollow nanogels are virtually nontoxic to A2780 cells.

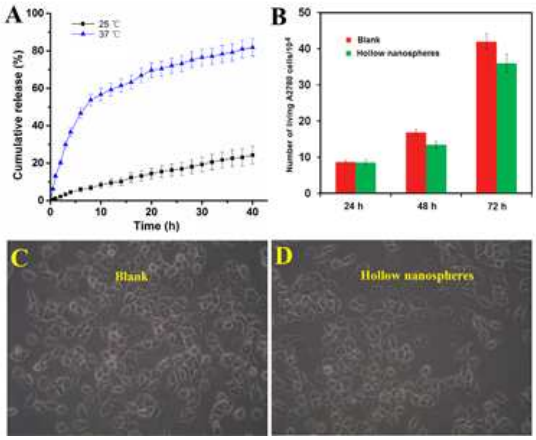

Fig. 6. Controlled release of DOX•HCl and cellular toxicity evaluation of hollow nanospheres. (A) Cumulative release curves of DOX•HCl-loaded hollow nanospheres at 25 °C and 37 °C; (B) number of living A2780 cells in the blank group after treatment with hollow nanospheres from day 1 to day 3; and images of living A2780 cells in the (C) blank and (D) hollow nanospheres groups after 72 h.

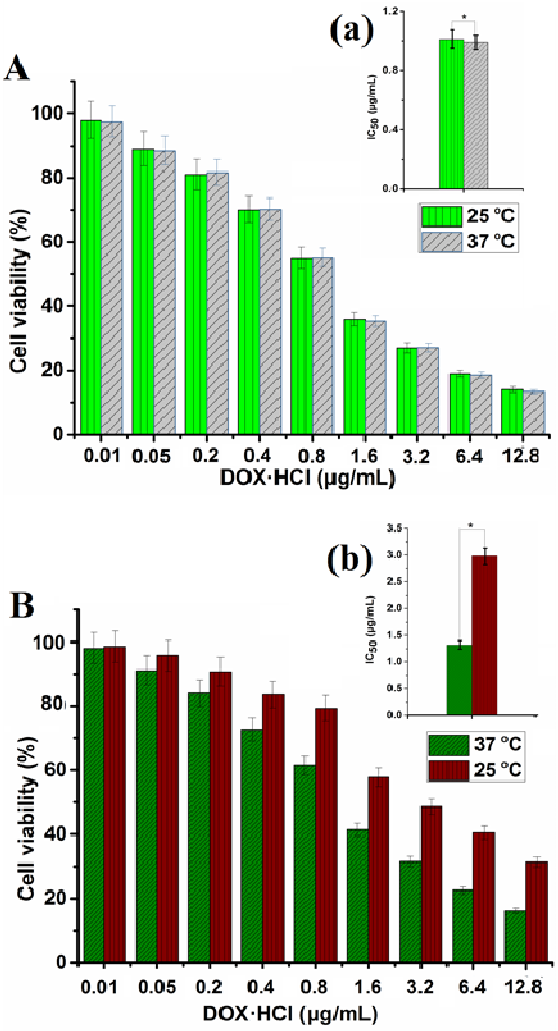

Fig. 7 In vitro cytotoxicity of free DOX•HCl (A) and DOX•HCl-loaded hollow nanospheres (B) at 37 and 25 °C, respectively, and the comparison of their IC_{50} values at different temperature (a and b). Data represent the mean ± standard deviation (SD) of 3 separate experiments. *p < 0.05 is statistically significant.

The in vitro cell viability of A2780 cells cultured with DOX loaded hollow nanospheres and free DOX•HCl molecules in the same drug concentration at both 37 °C and 25 °C were studied. As shown in Fig. 7A and B, no significant difference in cytotoxicity was found of free DOX•HCl at 37 °C and 25 °C, and the in vitro half maximal inhibitory concentration (IC_{50}) values of the free DOX•HCl are ca. 1.01 and 0.99 μg/mL at 37 and 25 °C, respectively. However, significantly greater cytotoxicity was observed when culturing cells with DOX•HCl -loaded hollow nanospheres at 37 °C than those of culturing cells at 25 °C, and the IC_{50} of DOX•HCl-loaded hollow nanospheres were 1.32 and 2.98 μg/mL at 37 and 25 °C, respectively. As shown in Fig. 6A and B, the release of DOX•HCl was faster at 37 °C than that at 25 °C, and blank hollow nanospheres showed much lower cytotoxicity, indicating that

the release of DOX•HCl was responsible for the enhanced cytotoxic activity. Therefore, it is reasonable to conclude that the higher cytotoxicity was attributed to the more rapid release of DOX•HCl from deformed hollow nanospheres.[50] It is also noted that hollow naospheres-mediated DOX • HCl formulation exhibited lower cytotoxicity to A2780 cells when compared with free DOX • HCl at the same DOX • HCl concentration. Similar results indicated that free drug is more potent in inhibiting cell proliferation than nanoparticle drug delivery system reported by other groups.[50-52] All these results suggest that the hollow nanospheres exhibit potential applications in drug delivery.

Conclusion

In summary, the photo-controlled host–guest interaction can improve the core removal method for the preparation of hollow polymer nanospheres. The dissociation of host–guest interaction between AZO and β-CD under 365 nm UV light irradiation can drive the removal of the core component. The prepared hollow nanospheres displayed a typical "breathing" characteristic. The hollow nanospheres exhibited controlled drug release behaviour triggered by its distinct "breathing" characteristic and good biocompatibility. The DOX•HCl -loaded hollow nanospheres showed a statistically higher cytotoxicity against A2780 cells at 37 °C than that at 25 °C. Thus, the photo-controlled host–guest interaction reported in this work is a simple, environment friendly and highly efficient method to prepare hollow polymer nanospheres as controlled drug delivery.

Acknowledgements: We would like to acknowledge the support of the National Science Foundations of China (No. 21274116 and No. 21374088) and National Training Programs of Innovation and Entrepreneurship for Undergraduate of China (No. 201510699228). W.T. thanks the grant from theProgram for New Century Excellent Talents of Ministry of Education (NCET-13-0476), the Key Laboratory Program of Science and Technology Coordinator Innovation Project of Shanxi Province of China (2013SZS17-P01), the Program of New Staff and Research Area Project of NPU (13GH014602) and the Fundamental Research Funds for the Central Universities (3102015ZY096).

References

1 R. M. Kramer, C. Li, D. C. Carter, M. O. Stone and R. R. Naik, *J. Am. Chem. Soc.,* 2004, **126,** 13282-1286.
2 Z. Zhong, Y. Yin, B. Gates and Y. Xia, *AdV. Mater.,* 2000, **12,** 206-209.
3 E. Amstad and E. Reimhult, *Nanomedicine,* 2012, **7**, 145.
4 J. G. Zhang, S. Q. Xu and E. Kumacheva, *J. Am. Chem. Soc.,* 2004, **126,** 7908.
5 X. W. Meng, J. Qin, Y. Liu, M. M. Fan, B. J. Li, S. Zhang and X. Q. Yu, *Chem. Commun.*, 2010, **46**, 643-645.
6 S. D. Miao, C. L. Zhang, Z. M. Liu, B. X. Han, Y. Xie, S. J. Ding and Z. Z. Yang, *J. Phys. Chem. C,* 2008, **112,** 774-780.
7 M. H. Li and P. Keller, *Soft Matter,* 2009, **5,** 927-937.
8 Z. Li, D. Xiong, B. Xu, C. Wu, Y. An, R. Ma and L. Shi, *Polymer,* 2009, **50,** 825-831.
9 R. P. Brinkhuis, F. P. J. T. Rutjes and J. C. M. Hest*, Polym. Chem.,* 2011, **2,** 1449-1462.
10 W. H. Chiang, V. T. Ho; W. C. Huang, Y. F. Huang, C. S. Chern and H. C. Chiu, *Langmuir,* 2012, **28,** 15056-15064.
11 F. Caruso, M. Spasova, A. Susha, M. Giersig and R. A. Caruso, *Chem. Mater.,* 2001, **13,** 109-116.
12 B. Mu, P. Liu, X. R. Li, P. C. Du, Y. Dong and Y. J. Wang, *Mol. Pharmaceutics,* 2012, **9,** 91-101.
13 H. Guo, Q. Guo, T. Chu, X. Zhang, Z. Wu and D. Yu, *J Mater Sci Mater Med.,* 2014, **25,** 121-129.
14 W. J. Tong and C. Y. Gao, *J. Mater. Chem.,* 2008, **18,** 3799-3812.
15 S. C. Thickett, N. Wood, Y. H. Ng and B. P. Zetterlund, *Nanoscale,* 2014, **6,** 8590-8594.
16 P.C. Du, H. Y. Yan, J. Zeng and P. Liu, *J. Mater. Chem. B,* 2013, **1,** 5298-5308.
17 K. Kamata, Y. Lu and Y. N. Xia, *J. Am. Chem. Soc.,* 2003, **125**, 2384-2385.
18 G. Y. Liu, H. F. Ji, X. L. Yang and Y. M. Wang, *Langmuir,* 2008, 24, 1019-1025.
19 H. L. Xu, Q. R. Jiang, N. Reddya and Y. Q. Yang, *J. Mater. Chem.,* 2011, **21,** 18227-18235.
20 G. Schneider and G. Decher, *Nano Lett.,* 2004, **4,** 1833-1839.
21 L. Gao, K. Zhang, B. Peng, Y. Shi and Y. M. Chen. *J. Polym. Sci. Pol. Phys.,* 2012, **50**, 323-327.
22 Z. M. Xing, C. L. Wang, J. Yan, L. Zhang, L. Li and L. S. Zha, *Soft Matter,* 2011, **7,** 7992-7997.
23 Y. Kang, K. Guo, B. J. Li and S. Zhang, *Chem. Commun.*, 2014, **50**, 11083-11092
24 S. H. Wang, Q. X. Shen, M. H. Nawaza and W. A. Zhang, *Polym. Chem.,* 2013, **4,** 2151-2157.
25 Q. Yan, Y. Xin, R. Zhou, Y. W. Yin and J. Y. Yuan, *Chem. Commun*., 2011, **47,** 9594-9596.
26 J. H. Liu, G. S. Chen, M. Y. Guo and M. Jiang, *Macromolecules,* 2010, **43,** 8086-8093.
27 H J. Zhang, Y. Xin, Q. Yan, L. L. Zhou, L. Peng, J. Y. Yuan, *Macromol. Rapid Commun.*, 2012, **33,** 1952-1957.
28 H. T. Zhang, X. D. Fan, W. Tian, R. T. Suo, Z. Yang, Y. Bai and W. B. Zhang, *Chem. Eur. J.,* 2015, **21,** 5000-5008.
29 Z. Yang, X. D. Fan, W. Tian, D. Wang, H. T. Zhang and Y. Bai, *Langmuir,* 2014, **30,** 7319-7326.
30 Y. Bai, X. D. Fan, W. Tian, D. T. T. Liu, H. Yao, Z. Yang, H. T. Zhang and W. B. Zhang, *Polym. Chem.,* 2015, **6,** 732-737.
31 R. J. Dong, B. S. Zhu, Y. F. Zhou, D. Y. Yan and X. Y. Zhu, *Angew. Chem. Int. Ed.,* 2012, **51,** 11633-11637.
32 S. Y. Yu, T. Azzam, I. Rouiller and A. Eisenberg, *J. Am. Chem. Soc.,* 2009, **131,** 10557-1066.

33 T. T. Nielsen, V. Wintgens, C. Amiel, R. Wimmer and K. L. Larsen, *Biomacromolecules,* 2010, **11**, 1710−1715.
34 C. H. Li, Z. H. Ge, H. W. Liu and S. Y. Liu, *J. Polym. Sci. Part A: Polym. Chem.,* 2009, **47**, 4001-4013.
35 X. C. Yang, N. N. Zhaoa and F. J. Xu, *Nanoscale*, 2014, **6**, 6141-6150.
36 R. J. Dong, Y. Liu, Y. F. Zhou, D. Y. Yana and X. Y. Zhu, *Polym. Chem.,* 2011, **2,** 2771-2774.
37 X. Ma and Y. L. Zhao, *Chem. Rev.,* 2015, **115,** 7794-7839.
38 P. Xu, E. A. Van Kirk, W. J. Murdoch, Y. Zhan, D. D. Isaak, M. Radosz and Y. Shen. *Biomacromolecules,* 2006, **7,** 829-835.
39 P. Dutta, S. Shrivastava and J. Dey, *Macromol Biosci.,* 2009, **9,** 1116-1126.
40 J. X. Ding, X. L. Zhuang, C. S. Xiao, Y. L. Cheng, L. Zhao, C. L. He, Z. H. Tang and X. S. Chen, *J. Mater. Chem.,* 2011, **21,** 11383-11391.
41 Z. B. Qin, D. S. Guo, X. X. Gao and Y. Liu, *Soft Matter,* 2014, **10,** 2253-22563.
42 K. K. Zhang, Z. Gui, D. Y. Chen and M. Jiang. *Chem. Commun.,* 2009, **41,** 6234-6236.
43 J. Z. Du and S. P. Armes, *J. Am. Chem. Soc.,* 2005, **127,** 12800-12801.
44 X. Y. Liu, M. Jiang, S. L. Yang, M. Q. Chen, D. C. Chen, C. Yang and K. Wu, *Angew. Chem. Int. Ed.,* 2002, **41,** 2950-2953.
45 M. Heskins and J. E. Guillet, *J. Macromol. Sci.,* 1968, **2,** 1441-1455.
46 Y. Kang, Y. Ma, S. Zhang, L. S. Ding, and B. J. Li, *ACS Macro Lett.*,**2015**, *4*, 543–547.
47 S. Nayak, D. Gan, M. J. Serpe and L. Lyon, Small, 2005, **1,** 416–421.
48 G. Q. Liua, C. L. Zhu, J. Xu, Y. Xin, T. T. Yang, J. Li, L. Shi, Z. G. Guoa and W. M. Liu, Colloids Surf. B Biointerfaces. 2013, **111,** 7-14.
49 M. V. Putz, Carbon Bonding and Structures: Advances in Physics and Chemistry, Springer Science & Business Media, 2011. pp. 112-115.
50 Y. X. Cheng, Jing Hao, L. A. Lee, M. C. Biewer, Q. Wang, and M. C. Stefan, *Biomacromolecules,* 2012, **13,** 2163−2173.
51 J. Z. Du, L. Y. Tang, W. J. Song, Y. Shi and J. Wang, *Biomacromolecules,* 2009, **10,** 2169−2174.
52 Y. L. Li, L. Zhu, Z. Liu, R. Cheng, F. Meng, J. H. Cui, S. J. Ji, and Z. Zhong, *Angew. Chem., Int. Ed.,* 2009, **48,** 9914−9918.

Journal of Materials Chemistry B

GRAPHICAL ABSTRACT

Photo-controlled host–guest interaction as a new strategy to improve the preparation of "breathing" hollow polymer nanospheres as controlled drug delivery

Received 00th January 20xx,
Accepted 00th January 20xx

DOI: 10.1039/x0xx00000x

www.rsc.org/

Haitao Zhang, Wei Tian*, Rongtian Suo, Yang Yue, Xiaodong Fan, Zhen Yang, Hui Li, Wanbin Zhang, Yang Bai

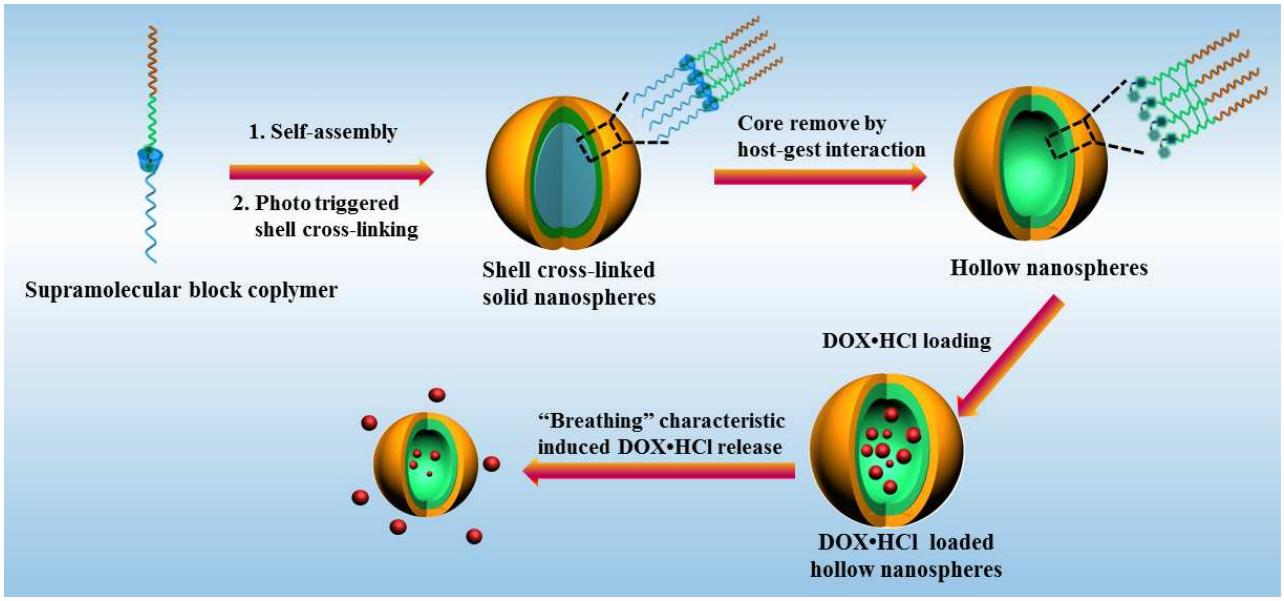

Photo-controlled host-guest interaction between azobenzene (AZO) and β-cyclodextrin (β-CD) as a new strategy is proposed to improve core removal method for preparing Poly((itaconoyloxy)ethyl methacrylate)-block-Poly(N-isopropylacrylamide) (PIEMA-*b*-PNIPAM)-based hollow nanospheres by three steps including construction of supramolecular block copolymer *via* host-guest interaction between AZO and β-CD, preparation of shell cross-linked solid nanospheres, and removal of core component by dissociation of host-guest interaction again. The prepared hollow nanospheres display a typical "breathing" characteristic, which can further induce the controlled release of doxorubicin hydrochloride (DOX•HCl).

[a] *The Key Laboratory of Space Applied Physics and Chemistry, Ministry of Education and Shanxi Key Laboratory of Macromolecular Science and Technology, School of Science, Northwestern Polytechnical University, Xi'an, 710072 (P. R. China)*
E-mail: happytw_3000@nwpu.edu.cn